Published in final edited form as:
Neurosurg Focus. 2010 September ; 29(3): E6. doi:10.3171/2010.5.FOCUS10120.

Emerging clinical imaging techniques for cerebral cavernous malformations: a systematic review

Peter G. Campbell, MD[1], **Pascal Jabbour, MD**[1], **Sanjay Yadla, MD**[1], and **Issam A. Awad, MD**[2]

[1]Department of Neurosurgery, Thomas Jefferson University and Jefferson Hospital for Neuroscience, Philadelphia, PA

[2]Neurovascular Surgery Program, Division of Neurosurgery, Biological Sciences Division and the Pritzker School of Medicine, University of Chicago, Chicago, Illinois

Abstract

Cerebral cavernous malformations (CCM) are divided into sporadic and familial forms. For clinical imaging, T2-weighted gradient-echo sequences have been shown to be more sensitive than conventional sequences. Recently more advanced imaging techniques such as high-field and susceptibility-weighted magnetic resonance imaging has been employed for the evaluation of CCMs. Furthermore, diffusion tensor imaging and functional magnetic resonance imaging have been applied to the preoperative and intraoperative management of these lesions. In this paper, the authors attempt to provide a concise review of the emerging imaging methods utilized in the clinical diagnosis and treatment of CCMs.

Keywords

magnetic resonance imaging; cavernoma; cavernous malformations; susceptibility-weighted imaging; gradient echo; functional magnetic resonance imaging

Cerebral cavernous malformations (CCM) are present in roughly 0.5% of the population[17,44]. These lesions are made up of clusters of deformed vessels, lined by endothelium and filled with blood at various stages of thrombosis[12,20]. The annual risk of hemorrhage ranges from 0.7 to 1.1% per lesion per year[44]. Typically, patients with single lesions have a sporadic form of the disease, while those with multiple lesions (10–31% of all cases) often have an autosomal dominant form localizable to the CCM1, CCM2 or CCM3 gene loci[7,18,28,32,45]. The hallmark of familial CCM is the presence of multifocal lesions throughout the brain with the appearance of new lesions over time[26]. The sporadic form of CCM is often characterized by a solitary lesion (or a cluster of lesions) in association with a DVA[3].

Prior to the widespread use of MR imaging, CCMs were thought to be rare entities. Modern MR imaging sequences are highly sensitive for detecting CCMs as well as associated hemorrhage at various stages of thrombosis and reorganization[30]. Typically, T2-weighted sequences portray these lesions as areas of mixed signal intensity, with a central complicated

Address correspondence to: Pascal Jabbour, MD, Department of Neurosurgery, 909 Walnut St, 2nd Floor, Philadelphia, PA 19107, pascal.jabbour@jefferson.edu.

Disclosure

The authors report no conflict of interest concerning the materials or methods used in this study or the findings specified in this paper.

IAA is supported by grant from the NIH/NINDS for research on cerebral cavernous malformation, including advanced imaging techniques (R01-NS060748).

core and a peripheral rim of decreased signal intensity[9,16]. T2-weighted gradient-echo (T2*GRE) imaging has been promoted as the gold standard MR imaging sequence for both sporadic and familial CCMs[30,54]. In the current study, we review the current literature and describe the use of emerging imaging techniques being utilized for the diagnosis and treatment of this entity.

Methods

The PUBMED and MEDLINE databases were searched for publications from 1966 to the present using MeSH terms “cavernoma”, “cavernous malformation”, “imaging”, “diffusion tensor imaging”, “susceptibility weighted”, “gradient echo”, “functional MR imaging”, “Tesla” and “High field MR imaging”. The search was limited to articles in the English language and relating to human subjects. Reference sections of recent articles and reviews were reviewed and pertinent articles identified. Initially, relevant articles were retrieved in abstract format. Full-text manuscripts were subsequently obtained for all original articles applicable to the current review. The review was supplemented by work currently in progress at the authors’ institutions.

Results and Discussion

Conventional MRI Features of CCM

Conventional MRI sequences (T1- and T2-weighted imaging) have been associated with the ability to identify clinically symptomatic CCM lesions with a specificity and sensitivity nearing 100%[42]. Many CCMs have a characteristic MR imaging appearance which includes a peripheral ring of hypointensity secondary to hemosiderin deposition in the surrounding parenchyma from repeated micro-hemorrhages[43]. Some authors describe this manifestation as an imaging appearance associated with a limited differential diagnosis[19]. A classification system based on imaging and pathologic features has been reported to stratify these heterogeneous lesions[54]. Type I lesions are characterized by hyperintensity on both T1- and T2-weighted images (depending on the state of methemoglobin) which is consistent with subacute hemorrhage[16]. In Type II malformations, loculated regions of hemorrhage are surrounded by gliosis and hemosiderin-stained brain parenchyma. These CCMs exhibit a mixed-signal intensity core on both T1- and T2-weighted images, with a well-circumscribed hypointense rim on T2-weighted imaging, and are the classic CCM with a “popcorn” appearance and a predilection to produce recurrent symptoms[11]. Type III lesions demonstrate a core that is iso- or hypointense on T1-weighted sequences and hypointense on T2-weighted sequences as well as a rim that is hypointense on T2-weighted sequences, compatible with chronic resolved hemorrhage or hemosiderin within and surrounding the lesion. Type IV malformations are minute lesions often seen as punctate hypointense foci on GRE MR images. Pathologically, Type 4 lesions may represent capillary telangiectasias or early stage CCMs seen frequently in the familial form[33,43,54]. The appearance of CCM may vary by MR imaging sequence as a result of differential magnetic susceptibility of blood products at different ages within the lesion, and the surrounding hemosiderin ring (Fig. 1).

Contrast enhanced imaging is particularly useful in the diagnostic evaluation of CCM, and in clarifying differential diagnosis. The presence of an associated DVA is more likely to define the nongenetic nonfamilial form of the disease[3,20]. Also, the presence of an associated DVA may influence surgical decisions, especially with regard to surgical maneuvers aimed at avoiding injury to the DVA and consequences of venous ischemia. The concept of lesion cure with surgical resection must be tempered when resecting a solitary CCM but leaving behind an overt DVA (which could later contribute to CCM recurrence). Contrast enhancement may delineate patterns of overt enhancement consistent with other pathology than CCM, particularly tumors (homogeneous enhancement), or arteriovenous

malformation (serpiginous enhancement). Finally, punctate enhancement in association with CCM's on enhanced T1 images, without hemosiderin "blossoming" on T2*GRE sequences, has been suggested to represent capillary telangiectasia, most commonly reported in the pons as well as in the bed of DVAs[40].

Diagnosis of CCM - Gradient Echo

Areas of the brain containing hemosiderin-laden tissue demonstrate a more recognizable hypointensity on T2-weighted GRE than either T2-weighted conventional spin-echo (SE) or fast spin echo (FSE) MR sequences due to magnetic susceptibility effects[4,8,21,23]. As such, T2*-weighted GRE imaging has been recommended as the most sensitive technique to evaluate CCM lesions in both the sporadic and familial forms of the disease[30,54]. During an in-depth evaluation of 57 French families with a history of familial CCM, Labauge et al[27] found approximately 5% probability that conventional MR imaging, without a T2*GRE sequence, would fail to spot a CCM. Furthermore, these authors reported mean number of lesions per person was five on standard MR imaging, while on T2*GRE sequences, the mean number of lesions detected was 16 ($p<0.001$)[27]. Other authors have reported a higher sensitivity with T2*GRE when compared to other sequences as well[10,39]. In evaluating a 3 generation family with familial CCM, Lehnhardt et al.[30] compared standard T1-weighted and T2-weighted SE sequences to T2*GRE sequences and noted a dramatically improved sensitivity with regard to lesion number and disease extension. When evaluating CCMs in association with DVA, the T2*GRE sequences may exclude or better delineate associated CCMs (Fig. 2).

The advantages of T2*GRE must be tempered by the effect of hemosiderin "blossoming" which effectively increases the apparent size of the CCM lesion. Hence, lesions may appear to extend to a pial or ependymal surface by T2*GRE, while in fact they are surrounded by several millimeters of normal or simply hemosoiderin stained brain tissue. This is extremely important to realize when planning surgical approaches to lesions in brainstem, or other eloquent or deep-seated locations. Also, T2*GRE sequences often reveal multifocal lesions in the setting of elderly patients with hypertension and history stroke, and the lesions often are distributed in the same territory as hypertensive angiopathy, and should be differentiated in clinical context from CCM (Fig. 3). Currently, T2*GRE sequences are considered an essential adjunct to the MR imaging of CCM. They are the method of choice in the sensitivity of detection and diagnosis of CCM, but should be supplemented by other sequences for more precise lesion definition, and by careful differential diagnosis.

Emerging Concepts in CCM Imaging

High Field MR Imaging—At present, low-flow vascular malformations, such as CCMs, are most frequently evaluated with standard 1.5 Tesla MR imaging based upon hemosiderin-induced susceptibility effects, which cause signal cancellations visible on T2*GRE sequences[29]. With standard imaging techniques, roughly 30% of epilepsy patients are not found to have an underlying lesion; some authors have posited an improved detection of CCMs could aid in the identification of CCMs (causing cryptogenic seizures) not visualized at 1.5 T[22,46]. Several authors have investigated the imaging effects of high field MRI in both experimental and clinical settings[36,38,46,48,49]. Shenkar et al.[48,49] evaluated ex-vivo human CCMs and murine CCMs by high-resolution MRI at 9.4 or 14.1 T. The results obtained by using high-field MR imaging correlated with the histopathological findings using confocal microscopy, confirming angioarchitecture of CCMs at near histological resolution[48,49]. Novak et al.[36] reported a case of a 55 year old with a frontal hemorrhage, although at 1.5 Tesla the CCM was not apparent. When closely analyzed, the CCM appeared larger and signal loss was several times greater on 8 T MR images than on 1.5-T images[36]. Schlamann et al.[46] performed imaging on 10 consecutive CCM patients at 1.5 and 7 T. These authors

found one additional hypointensity which was not visible in the 1.5 T examination, and multiple new small hypointense lesions were detected at 7 T in a patient with familial CCM. However, because of increased susceptibility artifacts, these lesions appeared on average 11% larger in the 7 Tesla images[46]. Given that magnetic susceptibility artifact is known to increase with the field strength and is readily captured by T2*GRE, CCMs not readily apparent on 1.5-T MR imaging may become more decisively detectable with higher magnetic field strengths[1,2]. Furthermore, these authors assessed lesion prevalence at high field using SW imaging, and at lower field using GRE sequences[46]. As a result, it remains unknown if the increased sensitivity reported by those authors is attributable to high field per se, or to SW imaging sequences as discussed below.

Susceptibility-Weighted MR Imaging—The CCM lesions contain deoxyhemoglobin and hemosiderin, which causes susceptibility effects and a decrease in signal intensity on T2-weighted sequences. Susceptibility weighted imaging provides a new mode that is particularly suited for imaging vascular malformations as it is very sensitive to deoxyhemoglobin and iron content[6,53]. This sequence is assembled from both magnitude and phase images from a high-resolution, 3D velocity-compensated GRE sequence[41]. Currently, this method is believed to be the only imaging method capable of appropriately detecting nonhemorrhagic cavernomas and telangiectasias[38]. Lee et al.[29] were the first to describe the use of SW imaging for imaging cavernomas. These authors presented a series of 10 patients who underwent both T2-weighted and SW MR imaging and found that not only were the margins of the CCMs better delineated, by SW imaging also revealed 2 additional lesions that were not seen on T2-weighted images[29]. Cooper et al.[15] reported a case of a 59 year-old familial CCM patient in which SW imaging detected nearly triple the number of lesions compared to the T2*GRE sequences. Pinker et al.[38] evaluated 17 patients harboring CCMs with a standard 1.5 T MR imaging in comparison to a 3-T MR imaging which included the SW imaging sequences. In this series, the 3-T SW MR imaging found an additional 7 lesions in 6 patients; however, it is unclear whether these patients had sporadic or familial CCMs. In a recent study, based on 15 subjects with familial CCMs and a mean age of 34 years old, de Souza et al.[16] found the following average number of lesions per patient: 5.7 on T2-weighted imaging; 26.3 on T2*GRE imaging and 45.6 on SW imaging. Thus the number of lesions seen on SW imaging was 1.7 times higher than that of T2*GRE ($p=0.001$)[16]. In the largest study to date, 23 cases were assessed by the senior author (IAA) and colleagues in Montpellier, France, which confirmed nearly twice the number of lesions detected by SW imaging as compared to T2*GRE sequences; however, this phenomena was only observed in the 14 familial cases. In none of 9 cases with solitary CCM or clustered lesions in the bed of a DVA did the SW imaging recognize additional lesions other than those noted on T2*GRE images (Menjot, et al., manuscript in preparation). Hence, SW imaging seems to increase the sensitivity of lesion detection in familial multifocal CCM lesions, it does not per se appear to reveal lesion multiplicity that had not been already demonstrated by T2*GRE (Figs. 4 and 5). The SW images are highly sensitive to delineation of associated venous anomalies, and possibly telangiectasias, without the need for contrast enhancement. This feature may be a significant advantage in pregnant patients, those with renal impairment and patients with allergic reactions to Gd-based contrast agents.

While SW imaging is not yet widely available it is possible that, given the early clinical data suggesting its effectiveness, it may be added into the routine imaging assessment of vascular malformations as improvements in software technology allow its acquisition and dissemination. These sequences might provide endophenotypic markers of disease burden in familial CCM that should be correlated with disease penetrance and aggressiveness in different individuals and kindreds, and with the response to potential therapeutic interventions.

The ultimate applicability of SW imaging is limited by several factors. First, as with T2*GRE, it is difficult to differentiate small venous structures from small hemorrhage and thrombosis. However, sequential SW imaging before and after Gd administration, could ameliorate this deficiency[31]. As previously noted, the higher sensitivity of SW sequences may not apply to sporadic or solitary CCMs, or CCM clusters associated with DVA. While SW imaging has shown greater ability to identify lesions in familial CCM, the necessity to apply this imaging modality to sporadic CCMs has yet to be demonstrated. We are not aware of a case in which a solitary lesion was detected on T2*GRE that was later found to be associated with occult lesion multiplicity on the more sensitive SW imaging (Fig. 5). As such, future studies should specifically address SW imaging sensitivity in cases of sporadic CCM, those associated with DVA and radiation induced CCMs.

Finally, the nature of those lesions which are delineated on SW imaging and remain occult on T2*GRE remains unclear (Fig. 4). Some may be better resolved in the 3D sequence acquisition of SW imaging, while they may have been diminished by “volume averaging” in the typically 2D acquisition of T2*GRE images. The occult punctate lesions may also represent non-hemorrhagic capillary telangiectasias, often reported in conjunction with CCM, which could also represent precursors to more mature CCMs[5].

Imaging in Intraoperative Management

The Use of Diffusion Tensor Imaging—Diffusion tensor imaging is an MR imaging technique that may be effectively used to visualize the directionality and orientation of white matter tracts in the brain[37]. Diffusion tensor tractography has been effectively used to evaluate the characterics of the hemosiderin rim surrounding CCMs as well as in surgical planning for the resection of CCM in eloquent areas[11,13,14,35]. Cauley et al[11] performed DT tractography on 18 patients with solitary CCMs and found that white matter tracts deviated around the center of CCMs, often passing through the hemosiderin rim. Niizuma et al[35] successfully utilized DT with fiber tracking to determine the location of the displaced corticospinal tract in the removal of a paraventricular CCM. Chen et al[13,14] have reported the used of DT imaging for the removal of several brainstem lesions including a CCM. They reported DT fiber tracking revealed the anatomical relationship between the local eloquent tracts and the CCM, thus altering their approach and preventing patient morbidity[14]. Several authors speculate DTI may be a useful preoperative imaging evaluation for patients with deep-seated lesions impinging upon white matter tracts[14,35]. Thus, the use of DTI may enhance the decision making process in the selection of surgical approaches by providing an enhanced understanding the relevant functional tracts.

Use of fMR Imaging—Functional MR imaging has the ability to integrate anatomic and functional information. Preoperatively, this imaging technique has the capacity to provide a useful representation of both task-related hemodynamic changes in the associated cortical area as well as the pathology through a single imaging modality[25]. An early case report described the successful use of fMR imaging in the preoperative assessment of a left central CCM[34]. Thickbroom et al[52] evaluated blood-O_2-level-dependent contrast fMR imaging in 3 CCM patients and noted some difficulty in correctly isolating the critical regions of eloquent cortex secondary to the associated susceptibility effect. Schlosser et al[47], working with the senior author (I.A.A.), did not report any such difficulty. These authors continue to utilize fMR imaging in clinical practice, even in cases with recent bleeding (Fig. 6). The data from fMR imaging is often supplemented by intraoperative mapping of sensorimotor sulcus by reversal of evoked potential amplitude or direct cortical stimulation[55]. Zotta et al.[56] used traditional MR imaging and fMR imaging fusion to aid in preoperative planning as well as intraoperative guidance. In this series, the authors achieved greater rates of seizure freedom in the group of CCMs in eloquent areas operated with the aid of fMR imaging as compared

to the group without this modality[56]. While fMR imaging has demonstrated a clear benefit over other modalities such as brain mapping or somatosensory evoked potentials for tumors located in primary motor cortex, more comprehensive studies to evaluate this technique in the setting of CCMs are needed[50]. Specifically, an improved outcome may be attributed to fMR imaging information, while in fact it was achieved because of a combination of information modalities. In CCM, functional data may affect the surgical route chosen to a lesion, and also the extent of resection of perilesional epileptogenic brain in cases with intractable epilepsy[24,51,56].

Conclusions

Prior to the advent of MRI, evaluation of CCMs was limited to diagnostic angiography and CT. Currently, MR imaging is the best imaging method to evaluate CCMs, with T2*GRE sequences being described as the “gold standard.”[10,30,54] As the use of more advanced imaging techniques continues to achieve widespread distribution, high-field MR imaging and SW MR imaging are likely to become commonplace for the diagnosis and follow-up of these lesions. Additionally, applications such as DT imaging and fMR imaging may achieve more relevance as intraoperative navigational modalities for deep-seated lesions in eloquent areas.

Abbreviations used in the paper

CCM	cerebral cavernous malformation
DT	diffusion tensor
DVA	developmental venous anomaly
GRE	gradient echo
fMR	functional MR
SW	susceptibility weighted
T2*GRE	T2-weighted GRE

References

1. Abduljalil AM, Kangarlu A, Yu Y, Robitaille PM. Macroscopic susceptibility in ultra high field MRI. II: acquisition of spin echo images from the human head. J Comput Assist Tomogr. 1999; 23:842–844. [PubMed: 10589556]
2. Abduljalil AM, Robitaille PM. Macroscopic susceptibility in ultra high field MRI. J Comput Assist Tomogr. 1999; 23:832–841. [PubMed: 10589555]
3. Abdulrauf SI, Kaynar MY, Awad IA. A comparison of the clinical profile of cavernous malformations with and without associated venous malformations. Neurosurgery. 1999; 44:41–46. discussion 46–47. [PubMed: 9894962]
4. Atlas SW, Mark AS, Grossman RI, Gomori JM. Intracranial hemorrhage: gradient-echo MR imaging at 1.5 T. Comparison with spin-echo imaging and clinical applications. Radiology. 1988; 168:803–807. [PubMed: 3406410]
5. Awad IA, Robinson JR Jr, Mohanty S, Estes ML. Mixed vascular malformations of the brain: clinical and pathogenetic considerations. Neurosurgery. 1993; 33:179–188. discussion 188. [PubMed: 8367039]
6. Barnes SR, Haacke EM. Susceptibility-weighted imaging: clinical angiographic applications. Magn Reson Imaging Clin N Am. 2009; 17:47–61. [PubMed: 19364599]
7. Bergametti F, Denier C, Labauge P, Arnoult M, Boetto S, Clanet M, et al. Mutations within the programmed cell death 10 gene cause cerebral cavernous malformations. Am J Hum Genet. 2005; 76:42–51. [PubMed: 15543491]

8. Bradley WG Jr. MR appearance of hemorrhage in the brain. Radiology. 1993; 189:15–26. [PubMed: 8372185]
9. Brunereau L, Labauge P, Tournier-Lasserve E, Laberge S, Levy C, Houtteville JP. Familial form of intracranial cavernous angioma: MR imaging findings in 51 families. French Society of Neurosurgery. Radiology. 2000; 214:209–216. [PubMed: 10644126]
10. Brunereau L, Leveque C, Bertrand P, Tranquart E, Cordoliani Y, Rouleau P, et al. Familial form of cerebral cavernous malformations: evaluation of gradient-spin-echo (GRASE) imaging in lesion detection and characterization at 1.5 T. Neuroradiology. 2001; 43:973–979. [PubMed: 11760804]
11. Cauley KA, Andrews T, Gonyea JV, Filippi CG. Magnetic resonance diffusion tensor imaging and tractography of intracranial cavernous malformations: preliminary observations and characterization of the hemosiderin rim. J Neurosurg. 112:814–823. [PubMed: 20367384]
12. Challa VR, Moody DM, Brown WR. Vascular malformations of the central nervous system. J Neuropathol Exp Neurol. 1995; 54:609–621. [PubMed: 7666048]
13. Chen X, Weigel D, Ganslandt O, Buchfelder M, Nimsky C. Diffusion tensor imaging and white matter tractography in patients with brainstem lesions. Acta Neurochir (Wien). 2007; 149:1117–1131. discussion 1131. [PubMed: 17712509]
14. Chen X, Weigel D, Ganslandt O, Fahlbusch R, Buchfelder M, Nimsky C. Diffusion tensor-based fiber tracking and intraoperative neuronavigation for the resection of a brainstem cavernous angioma. Surg Neurol. 2007; 68:285–291. discussion 291. [PubMed: 17719968]
15. Cooper AD, Campeau NG, Meissner I. Susceptibility-weighted imaging in familial cerebral cavernous malformations. Neurology. 2008; 71:382. [PubMed: 18663188]
16. de Souza JM, Domingues RC, Cruz LC Jr, Domingues FS, Iasbeck T, Gasparetto EL. Susceptibility-weighted imaging for the evaluation of patients with familial cerebral cavernous malformations: a comparison with t2-weighted fast spin-echo and gradient-echo sequences. AJNR Am J Neuroradiol. 2008; 29:154–158. [PubMed: 17947370]
17. Del Curling O Jr, Kelly DL Jr, Elster AD, Craven TE. An analysis of the natural history of cavernous angiomas. J Neurosurg. 1991; 75:702–708. [PubMed: 1919691]
18. Denier C, Goutagny S, Labauge P, Krivosic V, Arnoult M, Cousin A, et al. Mutations within the MGC4607 gene cause cerebral cavernous malformations. Am J Hum Genet. 2004; 74:326–337. [PubMed: 14740320]
19. Dillon WP. Cryptic vascular malformations: controversies in terminology, diagnosis, pathophysiology, and treatment. AJNR Am J Neuroradiol. 1997; 18:1839–1846. [PubMed: 9403438]
20. Gault J, Sarin H, Awadallah NA, Shenkar R, Awad IA. Pathobiology of human cerebrovascular malformations: basic mechanisms and clinical relevance. Neurosurgery. 2004; 55:1–16. discussion 16–17. [PubMed: 15214969]
21. Haque TL, Miki Y, Kanagaki M, Takahashi T, Yamamoto A, Konishi J, et al. MR contrast of ferritin and hemosiderin in the brain: comparison among gradient-echo, conventional spin-echo and fast spin-echo sequences. Eur J Radiol. 2003; 48:230–236. [PubMed: 14652139]
22. Huang CW, Hsieh YJ, Tsai JJ, Pai MC. Cognitive performance in cryptogenic epilepsy. Acta Neurol Scand. 2005; 112:228–233. [PubMed: 16146491]
23. Kim JK, Kucharczyk W, Henkelman RM. Cavernous hemangiomas: dipolar susceptibility artifacts at MR imaging. Radiology. 1993; 187:735–741. [PubMed: 8497623]
24. Komotar RJ, Mikell CB, McKhann GM 2nd. “Epilepsy surgery” versus lesionectomy in patients with seizures secondary to cavernous malformations. Clin Neurosurg. 2008; 55:101–107. [PubMed: 19248674]
25. Krings T, Reinges MH, Erberich S, Kemeny S, Rohde V, Spetzger U, et al. Functional MRI for presurgical planning: problems, artefacts, and solution strategies. J Neurol Neurosurg Psychiatry. 2001; 70:749–760. [PubMed: 11385009]
26. Labauge P, Brunereau L, Levy C, Laberge S, Houtteville JP. The natural history of familial cerebral cavernomas: a retrospective MRI study of 40 patients. Neuroradiology. 2000; 42:327–332. [PubMed: 10872151]

27. Labauge P, Laberge S, Brunereau L, Levy C, Tournier-Lasserve E. Hereditary cerebral cavernous angiomas: clinical and genetic features in 57 French families. Societe Francaise de Neurochirurgie. Lancet. 1998; 352:1892–1897. [PubMed: 9863787]
28. Laberge-le Couteulx S, Jung HH, Labauge P, Houtteville JP, Lescoat C, Cecillon M, et al. Truncating mutations in CCM1, encoding KRIT1, cause hereditary cavernous angiomas. Nat Genet. 1999; 23:189–193. [PubMed: 10508515]
29. Lee BC, Vo KD, Kido DK, Mukherjee P, Reichenbach J, Lin W, et al. MR high-resolution blood oxygenation level-dependent venography of occult (low-flow) vascular lesions. AJNR Am J Neuroradiol. 1999; 20:1239–1242. [PubMed: 10472978]
30. Lehnhardt FG, von Smekal U, Ruckriem B, Stenzel W, Neveling M, Heiss WD, et al. Value of gradient-echo magnetic resonance imaging in the diagnosis of familial cerebral cavernous malformation. Arch Neurol. 2005; 62:653–658. [PubMed: 15824268]
31. Lin W, Mukherjee P, An H, Yu Y, Wang Y, Vo K, et al. Improving high-resolution MR bold venographic imaging using a T1 reducing contrast agent. J Magn Reson Imaging. 1999; 10:118–123. [PubMed: 10441013]
32. Liquori CL, Berg MJ, Siegel AM, Huang E, Zawistowski JS, Stoffer T, et al. Mutations in a gene encoding a novel protein containing a phosphotyrosine-binding domain cause type 2 cerebral cavernous malformations. Am J Hum Genet. 2003; 73:1459–1464. [PubMed: 14624391]
33. Maraire JN, Awad IA. Intracranial cavernous malformations: lesion behavior and management strategies. Neurosurgery. 1995; 37:591–605. [PubMed: 8559286]
34. Moller-Hartmann W, Krings T, Coenen VA, Mayfrank L, Weidemann J, Kranzlein H, et al. Preoperative assessment of motor cortex and pyramidal tracts in central cavernoma employing functional and diffusion-weighted magnetic resonance imaging. Surg Neurol. 2002; 58:302–307. discussion 308. [PubMed: 12504288]
35. Niizuma K, Fujimura M, Kumabe T, Higano S, Tominaga T. Surgical treatment of paraventricular cavernous angioma: fibre tracking for visualizing the corticospinal tract and determining surgical approach. J Clin Neurosci. 2006; 13:1028–1032. [PubMed: 17070685]
36. Novak V, Chowdhary A, Abduljalil A, Novak P, Chakeres D. Venous cavernoma at 8 Tesla MRI. Magn Reson Imaging. 2003; 21:1087–1089. [PubMed: 14684215]
37. Pierpaoli C, Jezzard P, Basser PJ, Barnett A, Di Chiro G. Diffusion tensor MR imaging of the human brain. Radiology. 1996; 201:637–648. [PubMed: 8939209]
38. Pinker K, Stavrou I, Szomolanyi P, Hoeftberger R, Weber M, Stadlbauer A, et al. Improved preoperative evaluation of cerebral cavernomas by high-field, high-resolution susceptibility-weighted magnetic resonance imaging at 3 Tesla: comparison with standard (1.5 T) magnetic resonance imaging and correlation with histopathological findings--preliminary results. Invest Radiol. 2007; 42:346–351. [PubMed: 17507804]
39. Porter PJ, Willinsky RA, Harper W, Wallace MC. Cerebral cavernous malformations: natural history and prognosis after clinical deterioration with or without hemorrhage. J Neurosurg. 1997; 87:190–197. [PubMed: 9254081]
40. Pozzati E, Marliani AF, Zucchelli M, Foschini MP, Dall'Olio M, Lanzino G. The neurovascular triad: mixed cavernous, capillary, and venous malformations of the brainstem. J Neurosurg. 2007; 107:1113–1119. [PubMed: 18077947]
41. Reichenbach JR, Haacke EM. High-resolution BOLD venographic imaging: a window into brain function. NMR Biomed. 2001; 14:453–467. [PubMed: 11746938]
42. Rigamonti D, Johnson PC, Spetzler RF, Hadley MN, Drayer BP. Cavernous malformations and capillary telangiectasia: a spectrum within a single pathological entity. Neurosurgery. 1991; 28:60–64. [PubMed: 1994283]
43. Rivera PP, Willinsky RA, Porter PJ. Intracranial cavernous malformations. Neuroimaging Clin N Am. 2003; 13:27–40. [PubMed: 12802939]
44. Robinson JR, Awad IA, Little JR. Natural history of the cavernous angioma. J Neurosurg. 1991; 75:709–714. [PubMed: 1919692]
45. Sahoo T, Johnson EW, Thomas JW, Kuehl PM, Jones TL, Dokken CG, et al. Mutations in the gene encoding KRIT1, a Krev-1/rap1a binding protein, cause cerebral cavernous malformations (CCM1). Hum Mol Genet. 1999; 8:2325–2333. [PubMed: 10545614]

46. Schlamann M, Maderwald S, Becker W, Kraff O, Theysohn JM, Mueller O, et al. Cerebral cavernous hemangiomas at 7 Tesla: initial experience. Acad Radiol. 17:3–6. [PubMed: 19910215]
47. Schlosser MJ, McCarthy G, Fulbright RK, Gore JC, Awad IA. Cerebral vascular malformations adjacent to sensorimotor and visual cortex. Functional magnetic resonance imaging studies before and after therapeutic intervention. Stroke. 1997; 28:1130–1137. [PubMed: 9183338]
48. Shenkar R, Venkatasubramanian PN, Wyrwicz AM, Zhao JC, Shi C, Akers A, et al. Advanced magnetic resonance imaging of cerebral cavernous malformations: part II. Imaging of lesions in murine models. Neurosurgery. 2008; 63:790–797. discussion 797–798. [PubMed: 18981891]
49. Shenkar R, Venkatasubramanian PN, Zhao JC, Batjer HH, Wyrwicz AM, Awad IA. Advanced magnetic resonance imaging of cerebral cavernous malformations: part I. High-field imaging of excised human lesions. Neurosurgery. 2008; 63:782–789. discussion 789. [PubMed: 18981890]
50. Shinoura N, Yamada R, Suzuki Y, Kodama T, Sekiguchi K, Takahashi M, et al. Functional magnetic resonance imaging is more reliable than somatosensory evoked potential or mapping for the detection of the primary motor cortex in proximity to a tumor. Stereotact Funct Neurosurg. 2007; 85:99–105. [PubMed: 17228175]
51. Stavrou I, Baumgartner C, Frischer JM, Trattnig S, Knosp E. Long-term seizure control after resection of supratentorial cavernomas: a retrospective single-center study in 53 patients. Neurosurgery. 2008; 63:888–896. discussion 897. [PubMed: 19005379]
52. Thickbroom GW, Byrnes ML, Morris IT, Fallon MJ, Knuckey NW, Mastaglia FL. Functional MRI near vascular anomalies: comparison of cavernoma and arteriovenous malformation. J Clin Neurosci. 2004; 11:845–848. [PubMed: 15519860]
53. Wycliffe ND, Choe J, Holshouser B, Oyoyo UE, Haacke EM, Kido DK. Reliability in detection of hemorrhage in acute stroke by a new three-dimensional gradient recalled echo susceptibility-weighted imaging technique compared to computed tomography: a retrospective study. J Magn Reson Imaging. 2004; 20:372–377. [PubMed: 15332242]
54. Zabramski JM, Wascher TM, Spetzler RF, Johnson B, Golfinos J, Drayer BP, et al. The natural history of familial cavernous malformations: results of an ongoing study. J Neurosurg. 1994; 80:422–432. [PubMed: 8113854]
55. Zhou H, Miller D, Schulte DM, Benes L, Rosenow F, Bertalanffy H, et al. Transsulcal approach supported by navigation-guided neurophysiological monitoring for resection of paracentral cavernomas. Clin Neurol Neurosurg. 2009; 111:69–78. [PubMed: 19022559]
56. Zotta D, Di Rienzo A, Scogna A, Ricci A, Ricci G, Galzio RJ. Supratentorial cavernomas in eloquent brain areas: application of neuronavigation and functional MRI in operative planning. J Neurosurg Sci. 2005; 49:13–19. [PubMed: 15990714]

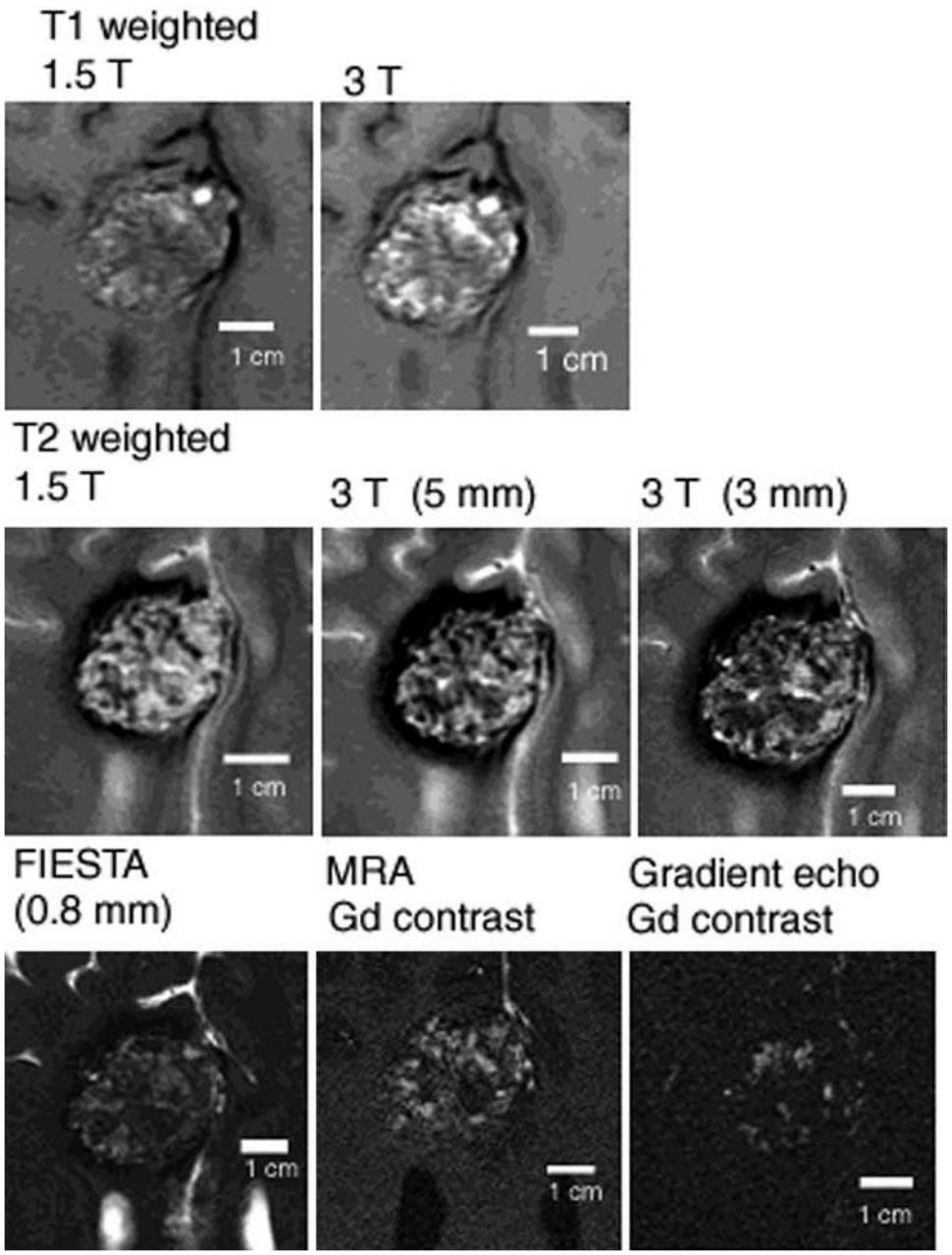

Fig. 1.

Subtle changes in appearance of solitary CCM with different MR imaging sequences, reflecting differential sensitivity of blood breakdown products at different ages, and low flow in dilated cavernous channels. The MR imaging appearance of human CCM lesions, including high field ex-vivo image correlations with confocal microscopy are presented in detail by Shenkar et al[49].

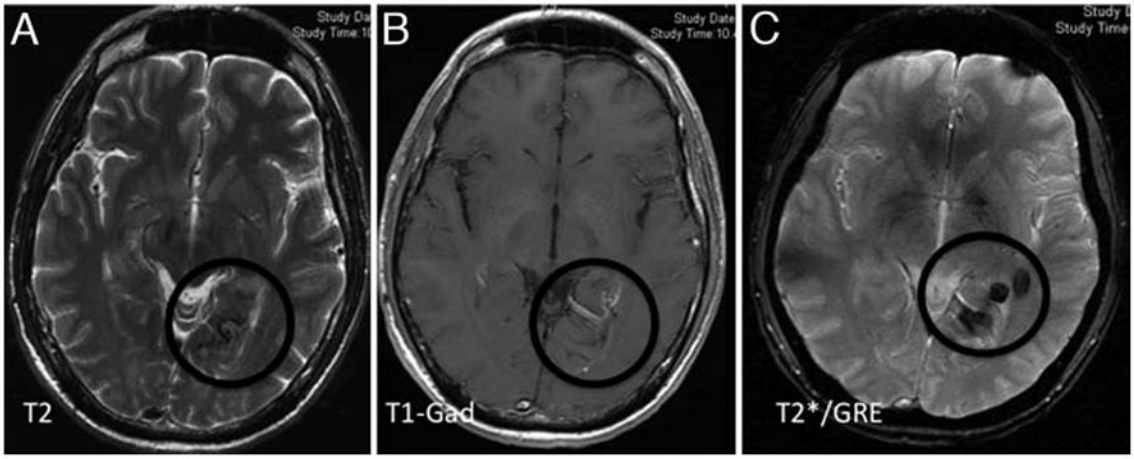

Fig. 2.

Multiple MR imaging sequences in a patient presenting with temporal lobe seizures. The T2-weighted sequence (A) illustrates subtle abnormality in the left posterior mesiotemporal region, consistent with non-specific hemosiderin deposition. The Gd-enhanced T1-weighted image (B) delineates a prominent venous structure with “caput medusae” pattern, associated with the T2-weighted signal, likely suggesting an associated DVA. The T2*GRE image (C) reveal much better delineation of multiple foci of CCM.

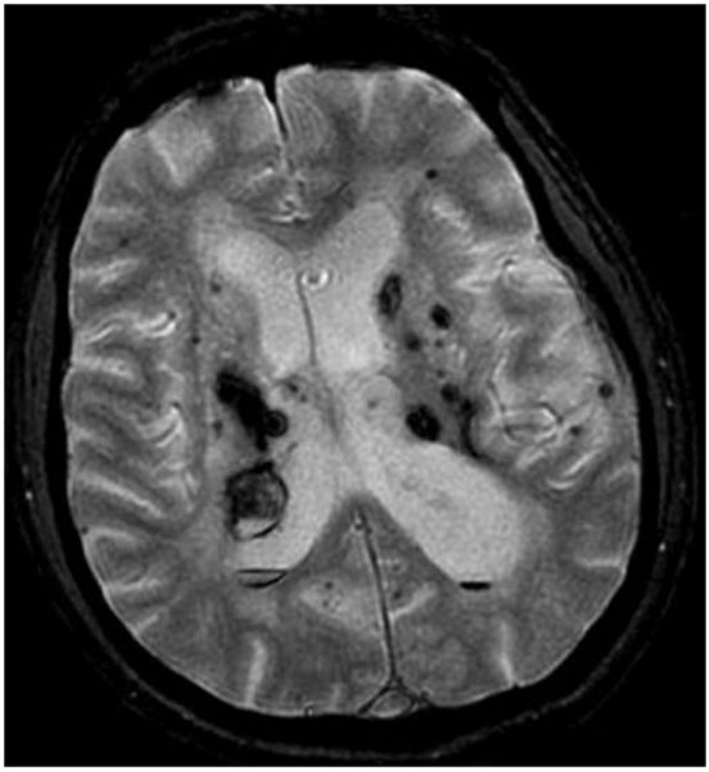

Fig. 3.

A T2*GRE MR image showing multifocal hemorrhagic lesions in an elderly patient with previous strokes, including recent intracerebral hemorrhages associated with untreated hypertension. The T2*GRE MR imaging sequences revealed multifocal occult tiny hemorrhagic lesions, interpreted as hypertensive angiopathy. These are differentiated from familial CCM disease by the clinical setting and by the clustering of lesions in periventricular areas most vulnerable to hypertensive angiopathy. Conversely, CCM disease is associated with lesions in a volume distribution throughout the brain.

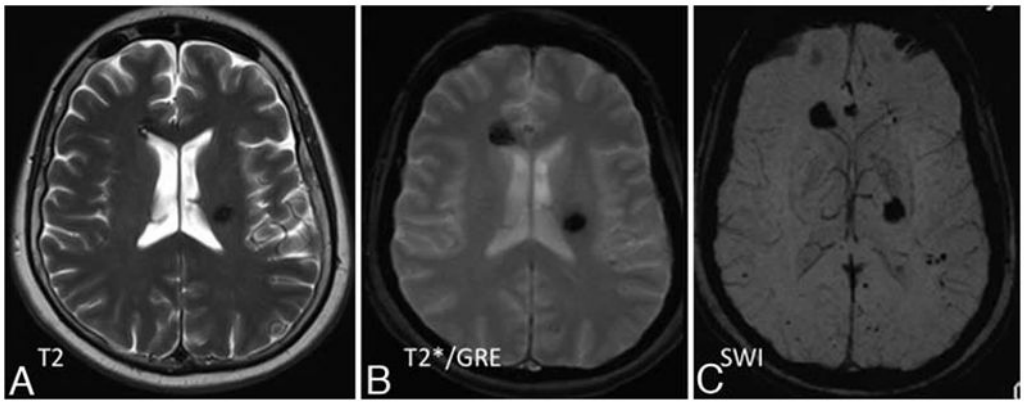

Fig. 4.

Representative T1-weighted (A), T2*GRE (B), and SW (C) MR images obtained in a patient with a family history of familial CCM disease, who presented for routine MR imaging screening. The T2 sequences (A) reveal 2 suspected CCM lesions, which were better delineated on T2*GRE sequences The T2*GRE sequences (B) also suggesting perhaps 1 or 2 additional subtle lesions. The SW images (C) reveal many additional lesions throughout the brain.

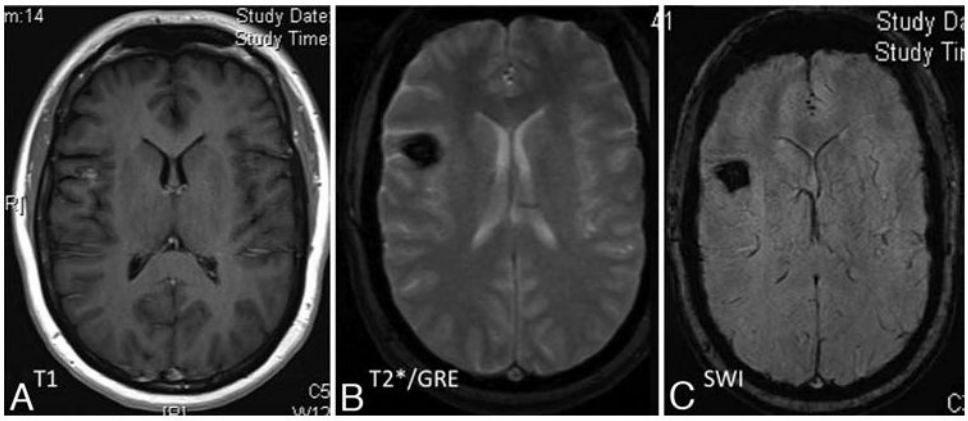

Fig. 5.

Representative T1-weighted (A), T2*GRE (B), and SW (C) MR images obtained in a patient with a solitary sporadic CCM that was discovered incidentally in the workup of an unrelated neoplasm. The T1-weighted contrast-enhanced images (A) revealed a suspected CCM in the right frontal cortex (left), and subtle abnormal venous prominence in superior and medial to the lesion (not shown). The T2*GRE images (B) better delineated the same lesion. The SW sequences (C) revealed no additional lesions, although they also demonstrate the suspected venous anomaly.

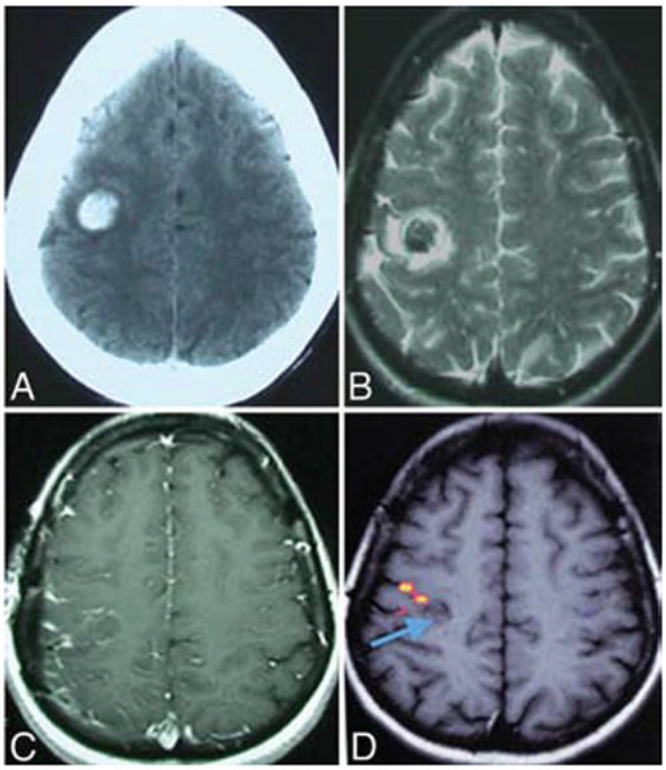

Fig. 6.

Representative CT scan an T2-weighted (B), T1-weighted (C), and functional (D) MR images obtained in a patient who presented with acute onset of left arm and hand paresis. The CT examination (A) revealed focal hemorrhage in the rolandic region. T2-weighted images (B) revealed a hemorrhagic lesion with surrounding edema, consistent with acute hemorrhage. The T1-weighed images (C) did not clearly clarify the location of sensorimotor structures in relation to the lesion. These were easily outlined by functional MR imaging (D), with zones of activation in response to left hand movement shown in *red-orange*. The region of functional activation on fMR imaging corresponded to reversal of somatosensory median nerve evoked sensory potential recording on the cortical surface, confirming the location of the rolandic sulcus. A more posterior sulcus was chosen for image-guided transsulcal microsurgical resection of the lesion (*blue arrow*), which proved to be a CCM, and the resection was accomplished without worsening in motor or sensory function.